TRI-DIMENSIONAL INVERSION OF SATELLITE MAGNETIC DATA FOR INDUCTION STUDIES

Pascal Tarits[1,2]

(1) IUEM, UMR CNRS 6538, Place Nicolas Copernic, F-29200 Brest, France, email: tarits@univ-brest.fr
(2) Earthquake Research Institute, OHRC, Yayoi 1-1-1, Bunkyo-ku, Tokyo 113-0032 Japan

ABSTRACT

A tri-dimensional (3-D) analysis of magnetic satellite data for induction studies is proposed. The data processing provides a series of external and internal Fourier and Spherical Harmonic coefficients of the magnetic potential. The potential is then modelled using a 3-D inversion scheme to retrieve the earth conductivity structure. The approach is tested on synthetic satellite data calculated for a magnetospheric inducing source and a 3-D heterogeneous conductivity model of the earth. .

1. INTRODUCTION

The purpose of the study presented in this paper is to demonstrate the feasability of 3-D conductivity inversion using satellite magnetic data. With the forthcoming of the *Swarm* constellation project for magnetic studies, a new era for global induction studies is opening with new ways to infer the electrical conductivity in the earth.

The situation is very unusual for induction studies as the transient magnetic field is sampled simultaneously both in time and space. It is however sampled at a high rate and continuously over the earth. Several studies have demonstrated the feasability of induction studies from space for simple source geometries and one dimensional (1-D) conductivity models (e.g. [1]]. The main objective of space induction is to obtain data to image the 3-D mantle conductivity. Studies to date suggest that a 3-D induction signal is present in the satellite data [2, 3]. Here, a full solution to this problem is tested. The first step consists of data processing to obtain observables suitable for conductivity modelling. The second step is modelling these observables to recover the 3-D conductivity structure. The approach is tested on synthetic magnetic data from [4].

2. DATA ANALYSIS

In the free space, at any time t, the vector magnetic field ***B*** may be described by a Fourier and a spherical harmonic expansion (FSHE) model of the form (see Appendix A for the definition of the SHE used here):

$$B^N(\hat{r}_t,t)=\sum_{l,m}\sum_{\omega} G^{Nm}_{l,\omega}(E,I)\,F^{Nm}_{l,\omega}(\theta_t,\varphi_t) \qquad (1)$$

The term r is the position vector. The coefficients E and I are the external and internal potentials at the degree and order l, m and frequency ω. For the sake of simplicity from now on l, m and ω are implicit in E and I values unless otherwise specified.

Eq. 1 is a linear system of the form $y=Ax$. The vector y contains the 3 components of the vector field ***B*** at all times t. The vector x is the vector of the potential coefficients E and I at all l, m and ω. The matrix A contains the FSH functions. The least-square solution of Eq. 1 is:

$$x=(A^*.A)^{-1}\ A^*y \qquad (2)$$

The matrix A^* is the Hermitian transposed of A. The term A^*y may be seen as a discrete estimate of the

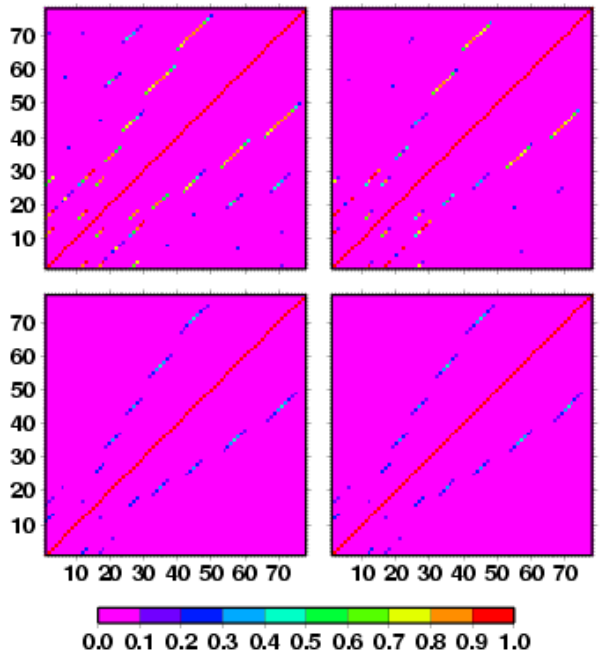

Figure 1 : The matrix R for 4 periods:12hrs (top left), 24hrs (top right), 2 days (bottom left) and 5 days (bottom right). The coefficients |Rij| are normalized by √RiiRjj to vary between 0-1. *The external coefficients E,are between l*=l-3 *and m=-l,l. They are numbered from n*=1-15 *(n=l*l+l+m). The internal coefficients I are between l*=1-7 *and m=-l,l. They are numbered from n*=16-78 *(n=15+l*l+l+m).*

general Fourier solution of Eq. 1 (Appendix B, Eqs. B-1-3). The resolution matrix $R=(A^*.A)^{-1}$ would reduce to a diagonal matrix if the field was sampled independantly in space and time (Eq. B-2). Because the satellite samples simultaneously the spatial and time variation of the magnetic vector $\boldsymbol{B}$, the resolution matrix contains off-diagonal terms expressing the coupling between the Fourier and SH coefficients. An exemple of the structure of the matrix R is presented in Fig. 1. A

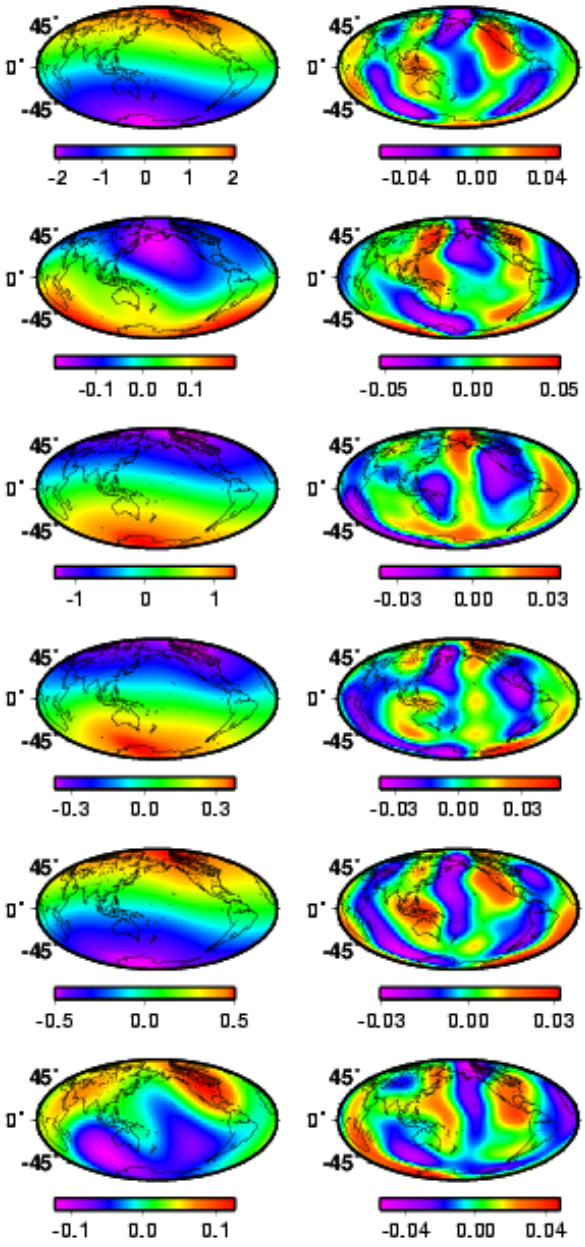

Figure 2: The E (left) and I (right) potentials are displayed in the space domain at four periods. For each period; the upper maps are the real part of the E and I porentials while the lower maps are the imaginary part.

SHE up to l=3 for the external field and up to l=7 for the internal field was used. The satellite rotation period and the earth rotation induce a strong aliasing effect at periods $\leq$1 day. The aliasing couples both space and time functions. The coupling is weaker at periods > 1 day. There is a numerical difficulty to analyse fully the structure of R. Even with a simplified source field structure, the task to describe fully the resolution matrix R becomes increasingly formidable as frequencies, degrees and orders are added to Eq. 1.

On earth, the external source field is roughly the result of 3 contributions, the magnetospheric ring current, the ionospheric solar variation and the field-aligned currents. The ionospheric source is internal with respect to the satellite. References [4] produced a series of simulation of the source field and its induction effect to study how to detect deep-seated regional conductivity anomalies. Three years of synthetic magnetic data were calculated for the future *swarm* constellation. The conductivity models of type I are a one-dimensional (1-D) mantle topped by the ocean/continent distribution. The type II conductivity models include additionnaly deep seated ad-hoc conductive bodies. The inducing sources may be magnetospheric only or may contained a ionospheric source as welll. The description of the data sets is found in [4] and will not be detailed here.

The synthetic satellite data used in this study are produced for a magnetospheric source only (with a SHE up to l=1 or l=1-3) and a conductivity model of type I. Such data cannot describe the full complexity of real data but this simplifies the data analysis to obtain the E and I terms of the SHE. They are extremely useful to test the approach proposed to derive the E and I potentiels.

One example is treated The number of frequencies as well as the number of degrees and orders l, m was limited to a small number. The SHE was limited to l=1-3, m=-l,l for the FSHE coefficients E, l=7, m=-l,l for the FSHE coefficients I. The Fourier spectra was obtained at 15 periods from 2-15 days. The data were analysed for successive 30 days long time series over one year. The results presented in this report are for the first set of 30 days of data.

The resulting E and I potentials are presented in Fig. 2 at a selection of 3 periods (15, 4 and 2.3 days). At each period, the SHE coefficients E and I are recombined into the E and I potentials in the space domain. The E potential is the SHE sum from l=1-3, m=-l,l while the I potential is the SHE sum from l=2-7, m=-l,l. The external field is correctly recovered at all periods for the real part (Fig. 2). The imaginary part is less stable than the real part at some periods where its amplitude is small. The internal potential I is calculated from l=2 to visualize the spatial geometry of the potential otherwise masked by the dominant l=1 term. The geometry of the

internal anomalous (i.e. induced by the conductivity heterogeneity) is complex but clearly controlled by the main conductivity contrasts (Fig. 2). In Fig. 3, some of the SH coefficients recovered using Eqs. 1-2 were compared to the original coefficients used to generate the synthetic data [4]. The processing of the synthetic satellite magnetic data provided in general fairly good estimates of the FSH coefficients. The best result was obtained for the dominant source field at l=1 and m=0 (Fig. 3).

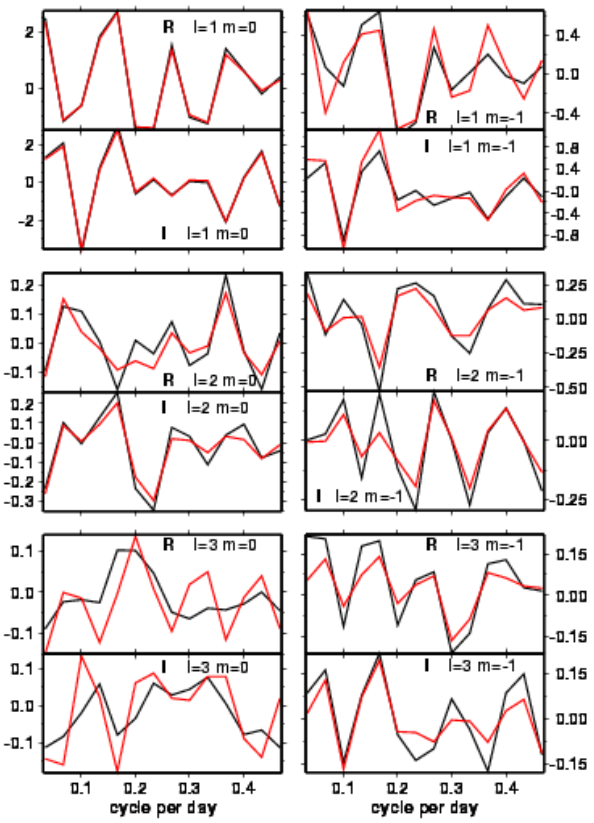

Figure 3 : SH coefficients E as a function of the frequency in cycle per day (1 cpd=11.57 μHz): in blue a the original coefficients used to produce the synthetic data.; in red, the coefficients obtained from the data analysis of the synthetic satellite data. The term R stands for real part and I for imaginary part.

3. INVERSION

The 3-D modelling of the electrical conductivity in the earth at the global scale implies the use of a 3-D spherical solver. Reference [4] generated the synthetic satellite data using the forward code proposed by [5]. In order to perform an inversion of these data, it is best to use a forward solver enterely different. The one used here [6,7] is based on a space/spectral approach. The conductivity is described by a stack of shells either homogeneous or heterogeneous. In each shell, the conductivity does not vary radially. The numerical solution is obtained by propagating the field both in space and spectral domains throughout the conductivity structure. The conductivity is never transformed into the SH domain. The forcing field is given by its SH coefficients and is applied at the earth surface. Since the E and I coefficients are obtained at the earth surface, there is no need to continue the computed field upward to satellite altitude.

The approach proposed here to invert the satellite data is based on the modelling of the potential coefficients recovered from the data analyis presented above. The coefficients have not been exactly recovered (Fig. 3). Furthermore, the data analysis may only provide a limited number of SH coefficients at a limited number of periods. The question therefore is whether or not such restricted number of coefficients carry enough information to recover the conductivity structure with a raisonnable degree of accuracy.

The inverse solution is seeked through the non-linear minimization of a misfit function between the observed and calculated coefficients I. The calculated FSHE coefficients I for a given conductivity model are obtained using the FSHE coefficients E as the inducing field in the forward solver.

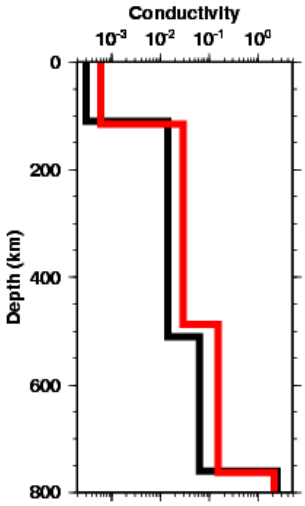

Figure 4: Best fitting model (in red) for the minimum misfit function between the FSHE internal coefficients I. The original 1-D structure beneath the heterogeneous upper shell used to synthetize the data is in black.

The inversion was carried out in two steps. First the best 1-D fitting model was obtained using the coefficients E and I up to l=3. The reason is for a 1-D conductivity model, I values exist only if there is a E value at the same degree and order. The 3-D solver was used for the inversion but with homogeneous layers. Fig. 4 shows the best fitting model compared to the mantle structure used in conductivity models of type I to generate the data.

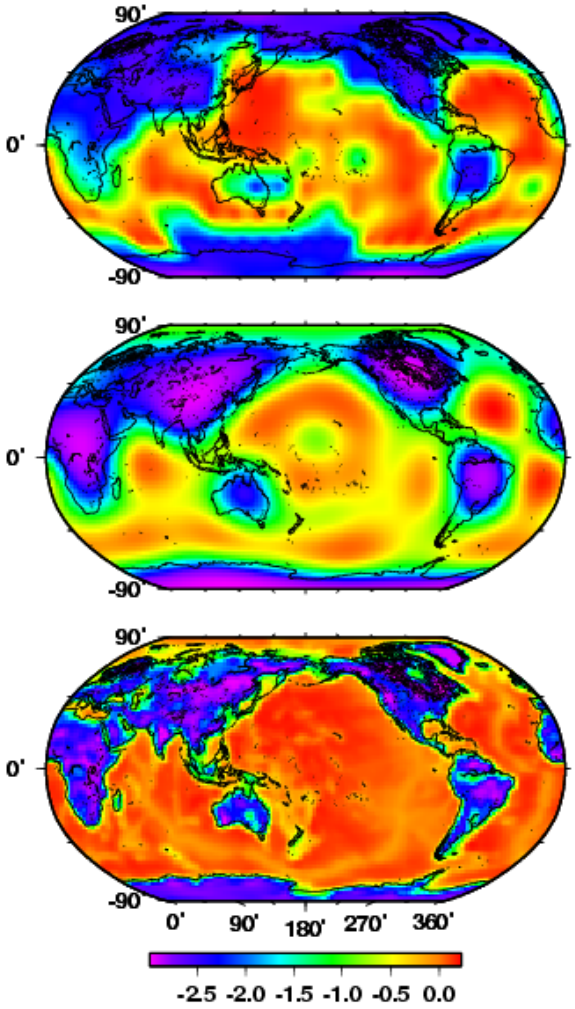

Figure 5: (Top) result of the 3-D inversion of the E and I data obtained from the synthetic satellite data. The color scale is the log of the electrical conductivity; (Bottom) the original full resolution (2x2°) layer used in synthetizing the satellite data; (Midde) the original conducitivity model low-pass filtered at l=8 for comparison with the result of the inversion (Top).

The second step started with this 1-D model and a homogeneous top layer (of conductivity 0.1 S/m) in which the conductivity in 200 meshes (20 in longitude and 10 in latitude) was ascribed to vary between 0.01 and 10 S/m. A good fitting model (after about 2000 iterations) is presented in Fig. 5 (top). This model compares well with the conductivity model in Fig.5 (middle) which is the original model (Fig. 5 bottom) low pass filtered to retain the structures at degrees *l* less than 8. The resulting conductivity model is quite good both in amplitude (conductivity values between 0.01-5 S/m) and in geometry. Some details are not correctly recovered though. Note that this inversion was run for a limited number of periods and SH calculated over the first segment of 30 days of satellite data. The extension to longer time series or the combination of more segments of similar time length is straitforward but time consuming. This is one of the next steps to carry on.

4. CONCLUSION

A general approach was proposed to process and invert satellite geomagnetic data to infer the 3-D conductivity of the earth. Both data analysis and inversion scheme were proved satisfactory to process synthetic data. While the approach presented here seems to work reasonnably well, it is only a partial answer to the question of magnetic data inversion for induction studies. A simple case with a pure magnetospheric source was considered. The inverse solution was seeked for the strong coast effect signal. Additional tests are needed including more data and estimating the improvement of the resulting model in accuracy. Then the satellite data synthetized with conductivity models of type II (with the mantle structures) should be considered as well as data including more realistic sources (namely including the ionosphere and the aligned currents). This set of tests could provide some interesting ideas to process the real data and be confident of the results.

5. REFERENCES

1. Olsen, N., Induction studies with satellite data, *Surveys in Geophysics*, 20, 309–340, 1999.
2. Tarits P., Preliminary investigation of the oersted data for induction studies, Oersted 3rd international Science team meeting, proceedings, 2000
3. Constable S.and C. Constable, Observing geomagnetic induction in magnetic satellite measurements and associated implications for mantle conductivity, *Geochemistry, Geophysics, Geosystems*, **5**, doi:10.1029/ 2003GC000,634, 2004.
4. Kuvshinov A, T. Sabaka, and N. Olsen, 3-D electromagnetic induction studies using the *Swarm* constellation: Mapping conductivity anomalies in the Earth's mantle *Earth Planets Space*, 58, 417–427, 2006.
5. Kuvshinov, A. V., D. B. Avdeev, O. V. Pankratov, S. A. Golyshev, and N. Olsen, Modelling electromagnetic fields in 3D spherical Earth using fast integral equation approach, in *3D Electromagnetics*, edited by M. S. Zhdanov and P. E. Wannamaker, chap. 3, pp. 43–54, Elsevier, Holland, 2002.
6. Tarits P., J. Wahr and P. Lognonné, Influence of conductivity heterogeneities at and near the CMB on the geomagnetic secular variation, AGU Fall meeting, 1998.
7. Grammatika N. and P. Tarits, Contribution at satellite altitude of electromagnetically induced anomalies from a 3-D heterogeneously conducting earth, Geophys. J. Int., 151, 3, 913-923., 2002

6. APPENDIX A

The spherical harmonic expansion (SHE) definition used throughout the paper is based on vectorial spherical harmonics [X]. The vector magnetic field is defined by $\boldsymbol{B}$ (B^+, B^0, B^-):

$$\begin{aligned} B^+ &= (B_\theta + iB_\varphi)/\sqrt{2} \\ B^0 &= B_r \\ B^- &= (-B_\theta + iB_\varphi)/\sqrt{2} \end{aligned} \qquad \text{A-1}$$

B_r, B_θ and B_φ are the usual spherical components of $\boldsymbol{B}$. The terms in Eq 1 are:

$$\begin{aligned} G_{l,\omega}^{Nm}(E,I) &= \varepsilon_l^N(r_t)\, E_l^{0m}(\omega) + \eta_l^N(r_t)\, I_l^{0m}(\omega) \\ F_{l,\omega}^{Nm}(\theta_t,\varphi_t) &= Y_l^{Nm}(\theta_t,\varphi_t)\, e^{i\omega t} \end{aligned} \qquad \text{A-2}$$

with N=-1, 0, +1. The Y^N terms are the vectorial SHE functions [X] and:

$$\begin{aligned} (\varepsilon^{-1},\varepsilon^0,\varepsilon^{+1}) &= (r/a)^{l-1}(-\Omega, l, -\Omega) \\ (\eta^{-1},\eta^0,\eta^{+1}) &= (a/r)^{l+2}(-\Omega, -l-1, -\Omega) \\ \Omega &= \sqrt{l(l+1)/2} \end{aligned} \qquad \text{A-3}$$

The value a is the earth's radius. As a result of A-3, the FSHE coefficients E and I, solution of Eqs. 1-2, are obtained at the earth's surface.

7. APPENDIX B

The FSHE coefficients E and I may be formaly obtained from the Fourier and Legendre inverse of Eq. 1:

$$(E_l^{0m}, I_l^{0m}) = \iint_{S,t} \sum_N (K_E^N, K_I^N) B^N \, ds\, dt \qquad \text{B-1}$$

where K_E and K_I are the kernels for E and I. The integrals are over the earth surface S and the time. When the space and functions are sampled at regular interval over S and a time length T, Eq B-1 is estimated with:

$$(E_l^{0m}, I_l^{0m}) = \sum_S \sum_T \sum_N (K_E^N, K_I^N) B^N \qquad \text{B-2}$$

For satellite data, the surface is sampled over time and the right-hand side of B-2 becomes:

$$\sum_{t,S(i)} \sum_N (K_E^N, K_I^N) B^N \qquad \text{B-3}$$